Published in final edited form as:
Mol Imaging. 2011 February ; 10(1): 3–16.

Inorganic Nanoparticles for Multimodal Molecular Imaging

Magdalena Swierczewska, **Seulki Lee**, and **Xiaoyuan Chen**
Laboratory of Molecular Imaging and Nanomedicine, National Institute of Biomedical Imaging and Bioengineering, National Institutes of Health, Bethesda, MD, and Department of Biomedical Engineering, Stony Brook University, Stony Brook, NY

Abstract

Multimodal molecular imaging can offer a synergistic improvement of diagnostic ability over a single imaging modality. Recent development of hybrid imaging systems has profoundly impacted the pool of available multimodal imaging probes. In particular, much interest has been focused on biocompatible, inorganic nanoparticle–based multimodal probes. Inorganic nanoparticles offer exceptional advantages to the field of multimodal imaging owing to their unique characteristics, such as nanometer dimensions, tunable imaging properties, and multifunctionality. Nanoparticles mainly based on iron oxide, quantum dots, gold, and silica have been applied to various imaging modalities to characterize and image specific biologic processes on a molecular level. A combination of nanoparticles and other materials such as biomolecules, polymers, and radiometals continue to increase functionality for in vivo multimodal imaging and therapeutic agents. In this review, we discuss the unique concepts, characteristics, and applications of the various multimodal imaging probes based on inorganic nanoparticles.

Inorganic nanoparticles offer many unique advantages for multimodal imaging owing to their unique size- and shape-dependent physical and chemical properties. Inorganic nanoparticles such as magnetic iron oxide nanoparticles (IONPs) are studied as magnetic resonance imaging (MRI) contrast agents,[1] semiconducting quantum dots (QDs) serve as optical probes for intracellular organelles and biomolecules,[2] metallic gold nanoparticles (AuNPs) exhibit unique light scattering patterns for surface-enhanced Raman spectroscopy,[3] and other particles exhibit unique properties useful for molecular imaging. The development of inorganic nanoparticles has grown tremendously owing to advances in synthesis methods and combination with other organic substances.[4] For the last 5 years, the number of publications for “inorganic nanoparticles” on the *ISI Web of Knowledge* database has increased steadily, totaling a 150% increase. This steady increase is mainly due to the discovery that these nanomaterials offer a unique high aspect ratio platform for multifunctionality, where multiple ligands such as targeting agents, drugs, and radioisotopes can be attached onto one particle for the possibility of molecular targeting, therapeutic delivery, and multimodal imaging.[5] Nanoparticles attached with targeting ligands can enter the cell and pursue specific biomolecules, giving it true molecular imaging capabilities. [6,7] As opposed to adjusting properties in bulk materials, nanoparticle shape and size are easily fine-tuned by the advances in lithography[8,9] and wet-chemistry[10,11] techniques offering tunable magnetic and optical properties for molecular imaging. The different components of the multifunctional nanomaterials can be synthesized in a heterogeneous manner,

Address reprint requests to: Xiaoyuan Chen, PhD, or Seulki Lee, PhD, Laboratory of Molecular Imaging and Nanomedicine, National Institute of Biomedical Imaging and Bioengineering, National Institutes of Health, Bethesda, MD 20892; Shawn.Chen@nih.gov; Seulki.Lee@nih.gov.

Financial disclosure authors and reviewers: None reported.

collectively encapsulated within a nanomaterial, or added onto a singular nanoplatform. Certain nanoparticle synthesis techniques require surface encasing materials to stabilize the nanoparticles and allow for dispersion.[12] The surface coatings can be modified with additional functional groups and multiple imaging agents for multimodal molecular imaging capabilities.

Molecular imaging characterizes the biologic functions of the body on the molecular level, allowing for a detailed understanding of the disease and an application of an individualized treatment to the patient. Standard molecular imaging systems commonly used in the clinic are positron emission tomography (PET), molecular MRI, and single-photon emission computed tomography (SPECT). Multimodal imaging combines the advantageous parameters of each individual modality into one system, allowing synergistic effects.[13–15] For example, the bimodal PET-MRI system incorporates the high sensitivity of PET with the high resolution of MRI, thereby circumventing the inherent low resolution of PET and low sensitivity of MRI.[16] Various molecular imaging techniques require different properties from probes, such as para- or superparamagnetic materials for MRI, radionuclides for PET and SPECT, high atomic number atoms for computed tomography (CT), and various fluorescent particles for optical imaging.[14] The multifunctionality of inorganic nanoparticles allows these properties to be delivered to the body in one tunable nanoplatform system. In this review, the advantages of inorganic nanoparticles and their unique characteristics for various multimodality imaging are discussed.

IONP-Based Multifunctional Probes

IONPs are superparamagnetic iron oxide crystalline structures that have the formula Fe_2O_3MO, where M is a divalent metal ion such as manganese, nickel, cobalt, or magnesium. Superparamagnetic iron oxide particles are made up of iron alone and have been extensively used as commercial T_2 MRI contrast agents such as Feridex, Resovist, and Combidex, with decreased toxicity compared to gadolinium (Gd)-based agents.[17,18] IONPs, along with their intrinsic superparamagnetic properties and therefore their promising application as a MRI contrast agent, can serve as nanoscaffolds for additional imaging probes for bimodal imaging.[19] The most widely used method to multifunctionalize IONPs is surface modification by covalent conjugation. Such particles are called cross-linked iron oxide (CLIO). The surface of the IONP can be crosslinked with other imaging probes, such as fluorophores for magnetic resonance (MR)-optical imaging and radionuclides for MR-PET imaging, as well as with targeting groups for specific therapies.

Optical absorption, luminescence, and fluorescence have also been combined with IONPs for the development of optical and MR contrast agents.[13] Although numerous visible light fluorescent probes have been combined with IONPs, such as rhodamine, fluorescein, and others, these probes prove ineffective in vivo owing to their limited tissue penetration property. Near-infrared (NIR) imaging is particularly useful because of the “biologic window.” This window refers to the 700 to 1,300 nm spectral region where blood, water, and tissue have reduced absorption and autofluorescence, allowing for agents that absorb and emit in the NIR to be easily detected. NIR dyes have been combined with IONPs to produce MRI–near-infrared fluorescence (NIRF) probes. CLIOs are chemically crosslinked dextran-coated IONPs that are widely accepted to be biocompatible owing to their stable hydrophilic polymer coating. Josephson and colleagues synthesized CLIO conjugated to the NIR dye Cy5.5 for dual MR and optical imaging.[20] Cy5.5 was conjugated to CLIO by amine groups on the dextran-coated IONP to the succinimidyl ester on the Cy5.5. This system has been repeated in numerous animal models ranging from sentinel lymph node (SLN) to brain tissue imaging, showing low cytotoxicity and multimodal functionality as MRI-NIRF imaging probes.[20,21]

In another embodiment, Santra and colleagues coencapsulated an NIR dye, dialkylcarbocyanine, and an anticancer drug, paclitaxel, into the poly(acrylic acid) (PAA) matrix on the surface of IONPs.[22] Carbodiimide chemistry and click chemistry were used to functionalize the surface of the PAA-IONP. This allowed versatility in the types of functional groups that can be used on the surface of IONPs, enhancing targeting and delivery of these molecular imaging and drug delivery probes. The probe is able to be (1) monitored by MRI and NIRF, (2) targeted to cancerous tissue by surface functionality, and (3) used to deliver an anticancer drug. Cellular uptake of the targeted probes was monitored by MRI relaxivity and NIRF, and induced cancer cell death was observed when paclitaxel was encapsulated within the PAA matrix. Such molecular imaging probes require a long circulation time and low uptake into the reticuloendothelial system (RES) to allow for accurate imaging.

Chen and colleagues developed an MRI-NIRF probe demonstrating high targeting specificity and low in vivo clearance by coating IONPs with a polyethylene glycol (PEG)-conjugated amphiphilic triblock copolymer made up of polybutylacrylate, polyethylacrylate, polymethacrylic acid, and octylamine.[23] A NIRF dye, IRDye800, and cyclic Arg-Gly-Asp-D-Tyr-Lys (cRGDyK) were further conjugated for NIR imaging and targeting for integrin $\alpha_v\beta_3$ receptors. Cyclic RGD analogues are peptides commonly used in nanoparticle engineering to target tumor integrin $\alpha_v\beta_3$ and in this example were shown to significantly improve tumor uptake of the bimodal imaging probe over non-RGD functionalized probes.[24] Successful tumor homing, as seen in this study in a subcutaneous U87MG glioblastoma xenograft model, gives true molecular imaging capabilities as a small amount of probes is required to obtain strong contrast enhancement at the site of imaging. The 20 nm diameter engineered particles exhibit increased circulation time owing to their PEG coating and reduced uptake by the liver.[23] PEGylation has been shown to increase circulation time in other nanomaterials, such as QDs, and may be applied to other nanoparticles to improve the biodistribution.[25,26] Recent works also demonstrated improved integrin $\alpha_v\beta_3$ receptor targeting with a copolymer coating between the targeting ligand and IONP. Chen and colleagues reported an amphiphilic diblock copolymer, poly(ethylene oxide)-block-poly(gamma-methacryloxypropyltrimethoxysilane) (PEO-b-PgammaMPS), which can be used to coat IONPs to reduce nonspecific cell and RES uptake because of its neutral charge.[27]

Beyond IONP conjugation to optical probes, numerous MRI-PET bimodal imaging agents have been developed with IONP as the main platform. An MRI-PET bimodal imaging system combines the sensitive molecular imaging of PET with the high-resolution imaging of MR. In this manner, the same molecular target can be imaged, evaluated, and analyzed with sensitivity and high resolution, giving anatomic and functional images. The design of an MRI-PET probe should involve proportionate amounts of each required material as MRI requires high doses of contrast agents, whereas PET uses only trace amounts. Radioisotopes for PET have been attached onto the IONP scaffold to provide dual-modality MR/PET imaging. Choi and colleagues designed a probe for MRI-PET made up of MnIONPs combined with the isotope ^{124}I.[28] MnIONPs have been shown to have T_2 relaxivity coefficients two to three times higher than IONPs without additional elements, therefore giving this hybrid nanoparticle a synergistic high MR contrast.[29] MnIONPs were first coated by serum albumin (SA) to prevent aggregation of the particles under physiologic conditions as well as to provide a binding point for the isotope. Second, ^{124}I binds directly to the tyrosine residue of SA. The authors demonstrated that the contrast enhancement of the conjugated isotope to the MnIONP did not differ from the contrast enhancement of the probes separately. ^{124}I-SA-MnIONP nanoparticles were verified in vivo to identify and distinguish the SLNs, giving both functional and anatomic information. SLN identification requires molecular imaging to determine if cancer has metastasized from its primary tumor

site, thereby enlarging the SLN.[28] The MR and PET imaging capabilities of the ^{124}I-SA-MnIONP are seen in Figure 1.

Another MRI-PET probe design incorporates DOTA chelated radionuclide ^{64}Cu on the IONP scaffold.[30] IONPs were coated with polyaspartic acid (PASP) through the carboxyl group, whereas the remaining amine group was used as a binding site for another linker, NHS-PEG-MAL, to conjugate cRGD and DOTA chelators on the surface. PASP and PEG, besides allowing conjugation of the PET probes onto the MRI probes, serve to stabilize the nanoparticles in physiologic conditions and reduce uptake through the RES, which is useful for long-term imaging. As this example suggests, linkers used to join two imaging inorganic probes together can be designed to improve in vivo capabilities. In this case, PASP linked the IONPs and radionuclide together and gave the bimodal probe enhanced tumor uptake and improved molecular imaging capabilities.

Although chemical linkers of imaging probes can themselves serve as multifunctional molecules, the composition of heterostructured nanoparticles for multimodal imaging provides a simpler approach to probe development. The combination of iron oxide with high absorbance agents, such as gold, has been used for bimodal optical absorbance sensing and MRI. Choi and colleagues synthesized various heterostructured nanoparticles made up of IONPs or MnIONPs and gold by thermal decomposition of the metal in surfactant complexes.[31] In particular, Au-Fe_3O_4 nanoparticles coated with a PEG-phospholipid shell and conjugated with 12-base oligonucleotide sequences showed an increase in T_2 contrast and red shift in the surface plasmon band. These probes were studied for both DNA sequence sensing and biomedical imaging. Complementary DNA binding self-assembly guided these particles to aggregate. During aggregation, the particles increase in size, as detected by dynamic light scattering, AuNP absorbance decreases and red shifts, and the T_2-weighted MRI contrast from the IONP decreases. The design of this system exemplifies that imaging by MR (IONPs) and optical absorbance (AuNPs) can be used for biosensing of specific DNA sequences and multimodal imaging.

Recently, Wang and Irudayaraj synthesized Fe_3O_4-Au-rod-Fe_3O_4 nanodumbbells and Fe_3O_4-Au-rod necklace-like particles that show variation in plasmonic and magnetic properties, which can be used for bimodal imaging.[32] The necklace-like probes are used as therapeutic, separation, and imaging agents because they can thermally ablate multiple pathogens such as *Escherichia coli* and *Salmonella typhimurium*, can be separated in solution by a simple magnet, and can be detected based on their ultraviolet/visible NIR absorbance, respectively.[32] However, this iron oxide/gold nanorod necklace example proposed in the literature was not used as a bimodal imaging agent even though IONPs have been highly studied for their MRI contrast enhancement. Au-Fe_3O_4 dumbbell-like nanoparticles have been synthesized and can be optically and magnetically detected.[33] The dumbbell shape allows versatility in the functionalization of each additional component. The Au particle was functionalized with PEG for increased circulation time in vivo, whereas the Fe_3O_4 component was functionalized with an epidermal growth factor receptor antibody linked via PEG and dopamine for human epithelial carcinoma cell line targeting.[33] Therefore, the nanoprobes were targeted to cancer cells while being detected by MRI and reflection imaging. By changing gold and iron oxide nanoparticle size and shape, the optical and magnetic properties can be fine-tuned. In fact, the T_2 times of IONPs were increased depending on the AuNP core size, even when the iron oxide concentrations stayed the same. The combination and design of hybrid inorganic molecules can serve to enhance or decrease imaging signals. Therefore, the interactions among inorganic molecules on the nanoscale must be thoroughly understood to engineer synergistic multimodal hybrid molecules.

IONPs, as seen by these previous examples, can serve as excellent scaffolds for additional imaging probes while maintaining the MRI capabilities. In this way, our laboratory has developed a multimodal imaging probe based on IONPs.[34] The nanoparticles were coated with human serum albumin (HSA), ^{64}Cu-DOTA, and Cy5.5 to allow for MRI, PET, and NIRF imaging for both in vivo and in vitro applications. A schematic image of the particle and imaging capabilities is shown in Figure 2. A key approach to this design is the addition of dopamine to the surface of the IONP, allowing the particles to be encapsulated within an HSA matrix. Once the particles are encapsulated within a molecular matrix, various drugs can be loaded within the matrix, giving it optimal drug release properties compared to covalent linking of the drug onto the particles. These particles not only envelop three different imaging modalities but also have excellent nanoparticle properties for in vivo applications: a prolonged circulation half-life, high accumulation within lesion sites, low uptake by macrophages, and a high extravasation rate.[34]

QD-Based Multifunctional Probes

QDs are semiconductors that are confined on the nanometer scale. At the reduced size, the oscillation strength is focused to a reduced number of transitions with electronic excitation shifts at higher energy.[35] The use of QDs for bioimaging arises from their unique optical properties, such as photostability, broad absorption sections, wide absorption spectra, and narrow emission spectra. These confined particles are used mainly as luminescence probes that have narrow, typically 20 to 30 nm full width at half maximum, and tunable emission spectra in the spectral range of 400 nm to 2 μm. The emission spectrum is tuned by the size of the confinement. For example, when the diameter of cadmium selenide (CdSe) is reduced from 20 nm to 2.0 nm, the band gap shifts from a deep red to a green color.[35] However, QDs can cause severe cytotoxicity when semiconductor leaching occurs, especially by cadmium (Cd), and the fluorescence emission has been reported to “blink.”[36] To overcome this limitation and improve multifunctionality of nanoparticles, a new class of biocompatible QDs has been reported. The recent development of various QD-based imaging probes has been described and reviewed elsewhere. [37–39] Besides the optical properties, QDs can also serve as scaffolds for additional imaging agents for the design of bimodal molecular probes.

By blending luminescent QDs and MRI contrast agents, enhanced probes can be designed for noninvasive MRI. Paramagnetic quantum dots (pQDs) were developed by coating CdSe/ZnS core/shell QDs with a PEGylated phospholipid and a Gd lipid, making the particles biocompatible and MRI active, respectively, without affecting the absorption and emission spectra of the QDs.[40] The synergistic effects of combining paramagnetic Gd with the semiconductor QDs show relaxivities at 2,000 $mM^{-1}s^{-1}$ per QD. The relaxivity of the pQDs at 60 MHz is 12 $mM^{-1}s^{-1}$ per Gd molecule, which is three times higher than the clinical contrast agent Gd-DTPA that coats the pQD. The pQDs were also conjugated by maleimide to cRGD for targeting angiogenic vascular endothelium as demonstrated by in vitro experiments with human umbilical vein endothelial cells.

In another example, fluorescence MRI bimodal agents were developed by doping silica nanoparticles with a QD coated with paramagnetic and PEGylated lipids.[41] In this way, surface functionalization steps where steric hindrance and coupling reactivity reduce the coating efficacy and form large variations in the ratio of materials covering the particle were avoided.[41] First, CdSe QDs were coated with seven monolayers of inorganic shells using successive ion layer adhesion and reaction (SILAR)[42] and then incorporated in silica spheres by reverse microemulsion to form silica-coated QDs. After purification of the silica synthesis reactants, the hydrophobic particles were coated with a densely packed monolayer of PEG-DSPE, MAL-PEG-DSPE, and Gd-DTPA-DSA. Then these water-stable particles were conjugated with cRGD via the Mal-PEG-DSPE coated on the surface of particles.

These particles can be detected by fluorescence with a 35% quantum yield and MRI with relaxivity of 14.4 $mM^{-1}s^{-1}$. Nontargeted particles had no significant MRI signal confirming that the target-specific molecular probes greatly improve molecular imaging.[41] A major disadvantage of using Cd-based QDs is cellular toxicity. But the doping of the QDs within silica particles may prevent or at least slow down the leaking of Cd in vivo. Current works with QDs stay away from the toxic Cd-based QDs and focus on silicon-based QDs.[43] Recently, paramagnetic silicon QDs doped with manganese (Si_{Mn} QDs) have been synthesized and are detectable by MRI and NIR excited two-photon imaging.[44] By doping Si QDs with a magnetic impurity, T_1-weighted relaxivity is 25.5 $mM^{-1}s^{-1}$, significantly higher than commercially available Gd contrast agents, and fluorescence is emitted at 441 nm at 8.1% quantum yield in water.[44] However, the synthesis of water-soluble Si_{Mn} QDs is complicated, involving oxygen-sensitive materials, high-energy milling, and high reaction temperature. Also, the QD two-photon emission spectra were red-shifted with increasing excitation wavelength, requiring sensitive data correction. To perform cellular studies, these probes were coated with dextran sulfate to target macrophages, as seen in Figure 3A. Compared to uncoated QDs, these probes accumulated in macrophages by a receptor-mediated process with limited toxicity. Strong fluorescence within the cell was verified to arise from the probes, and MRIs show a strong contrast between cell lysate with and without the SiMn QD probes, as seen in Figure 3B.

QDs have also been studied as MR and optical imaging contrast agents when combined with perfluorodecalin (PFD) synthesized into nanoemulsions.[45] InGaP/ZnS QDs dispersed in PFD (PDF/[InGaP/ZnS QDs]) were synthesized as nanoemulsions that contain ^{19}F molecules, which serve as ^{19}F-based MRI contrast agents.[45] This bimodal imaging agent can be delivered intracellularly into phagocytic and nonphagocytic immune cells without the use of transfecting agents and without affecting cell viability. By labeling such immune cells, which are involved in the early defense and elimination of tumor cells, immunotherapeutic strategies for preclinical or clinical cancer therapies can be applied. The important feature of these particles involves the exchange of the hydrophobic surface ligands of QDs with perfluorocarbons for proper mixing into the hydrophobic and lipophobic PFD to form nanoemulsions by phospholipid encapsulation. Figure 4A represents the synthesis process for these bimodal imaging agents.[45] The PDF/[InGaP/ZnS QDs] nanoemulsions exhibited bright red fluorescence (Figure 4B) and a ^{19}F-based MR signal when excited at the resonance frequency doublet peak (Figure 4C). Efficiency of intracellular delivery into macrophages was 91% with localization in the lysosome, whereas the efficiency for nonphagocytic cells was about 38%. No significant cytotoxicity was seen at 2% doses of PFD/QD nanoemulsions.

These MR and fluorescence imaging agents incorporate all requirements for a successful bimodal molecular imaging agent with good intracellular delivery, low cyotoxicity, and multifunctional targeted and sensing. Fluorescent core-shell CdSe/ZnS QDs can also be used as photoacoustic and photothermal microscopy contrast agents, as demonstrated by Shaskov and colleagues.[46] The core-shell CdSe/ZnS QDs have an absorption cross section in the visible and NIR range of 10^{-15} cm^2, about an order of magnitude better than other NIR fluorophores.[47] By adjusting the excitation laser pulse width, excited QDs can exhibit thermal energy, which can then be transformed into acoustic energy. Nanosecond pulse laser excitation at ranges between 420 and 900 nm is required to induce photoacoustic and photothermal effects.[46] QD photoacoustic and photothermal effects were not sensitive to scattering and autofluorescence background signals, but no in vitro images were taken.[46] A major problem with using high laser energies is the QD disintegration by core melting and explosion, leaving the potentially toxic semiconductors exposed in vitro and in vivo, as well as toxic bubble formation. Although numerous in vivo experiments have been performed

with QDs for targeting and fluorescence imaging,[36,48–52] few studies have been reported for bimodal imaging with QDs.

One example of bimodal in vivo work with QDs was shown by Cai and colleagues with the use of ^{64}Cu-labeled DOTA-QD-RGD conjugates in a U87MG tumor mouse model.[53] In this work, CdSe/ZnS QDs were modified with RGD peptides and ^{64}Cu-labeled DOTA for integrin $\alpha_n\beta_3$-targeted PET and NIRF imaging. Quantitative data by in vivo PET and ex vivo NIRF imaging were collected to determine the tumor targeting efficiency of these nanoparticles by both imaging modes with over 90% correlation, thereby overcoming tissue penetration limitations of optical imaging. About 4% injected dose per gram (% ID/g) was taken up by the tumor after 18 hours postinjection, an amount much higher compared to 1% ID/g by the nontargeted ^{64}Cu-labeled DOTA QDs. Both QD conjugates were shown to have high liver, spleen, lymph node, and bone marrow uptake. Over 50% ID/g liver uptake was seen for both DOTA-QD and DOTA-QD-RGD for all time points postinjection. A new direction following this study is to investigate the less toxic, non-Cd QDs for bimodal imaging.

Other Inorganic Nanoparticle–Based Multifunctional Probes

As seen by the silica nanoparticle QD doping example in the previous section, silica nanoparticles offer a variety of hybrid molecular imaging probes owing to their biologically inert surface and well-established loadable nanoplatform. [54] Silica particles can be used as shells for optically interesting core materials. For example, silica particles have been used to build luminescent and paramagnetic particles.[55] The core of the silica particle is filled with the luminescent, inner transition metal ruthenium, whereas a paramagnetic Gd monolayer coats the surface of the nanoparticle. The 37 nm diameter particles were synthesized using a well-controlled water-in-oil reverse microemulsion. A ligand-to-metal charge transfer is required for the ruthenium to show luminescence, with an absorption peak around 450 nm and emission at 595 nm. The nanoparticles were taken up by 98% of the monocyte cells with limited cytotoxicity. Laser scanning confocal microscopy was used to visualize the nanoparticles by the Ru luminescence, and T_1-weighted images showed significant contrast owing to the Gd doping. T_1 relaxivity is 19.7 $mM^{-1}s^{-1}$. Owing to the versatility of the platform, the multimodal imaging particle can be targeted to image specific diseases, such as rheumatoid arthritis in mice.[55]

Owing to their high absorbance and heating abilities, AuNPs have been used for photothermal therapy agents in the form of gold nanoshells, gold nanocages, and gold nanorods.[56–58] A 5 nm diameter AuNP has an absorption cross section of 3 nm^2 at 514 nm, which is twice as high as for a common organic fluorophore.[59] Owing to this high absorbance, AuNPs exhibit a photothermal effect, where an increase in temperature is exhibited around the particle when illuminated by light. Photothermal imaging depends on the detection of the temperature changes or the effects of that temperature change. Recent advances in photothermal imaging allow for the detection of slight phase changes owing to the increase in heat when the high absorbance particles are excited with laser light energy using a standard optical microscope.[60] Photoacoustic imaging is based on the photoacoustic effect. Just like the photothermal effect, the photoacoustic effect depends on the absorption of energy that is converted to heat. However, the heat energy leads to a thermoelastic expansion and emits as ultrasonic waves.[61] Photoacoustic imaging depends on detecting those ultrasonic emissions by ultrasonic transducers.[61] An advanced design of a fluorescence MRI nanoparticle also exhibits photothermal heating to induce cell death.[62] This type of particle is based on a gold nanoshell, thereby exhibiting photothermal capabilities, coated with a silica epilayer doped with the T_2 contrast agent iron oxide and organic fluorophore indocyanine green (ICG).[62] An interesting advantage to the design is a

significant fluorescence enhancement (45-fold) owing to the synergistic combination of all components. As proposed by the authors, the increased quantum yield can be attributed to the gold plasmon properties and its enhanced absorption. The particles were functionalized with anti-*HER2* antibodies and targeted to *HER2*-positive human breast cancer cells. Cell death of the targeted cells was seen when the cells were excited by NIR light owing to heating.[62]

Recently, gold was incorporated onto carbon nanotubes for efficient photoacoustic and photothermal signals and demonstrated hundred-time NIR contrast enhancement when used to map the lymphatic vessels in mice.[63] These so-called golden carbon nanotubes (GNTs) incorporate the properties of gold to act as NIR absorption enhancers by depositing a thin layer of gold around the carbon nanotubes. Not only are these GNTs adjustable in length, size, and thickness, they also exhibit minimal cytotoxicity. To study the photoacoustic and photothermal mapping in vivo, GNTs were conjugated with an antibody specific for the lymphatic endothelial hyaluronan receptor 1 (LYVE-1) for lymphatic endothelial cell mapping. Low laser fluence levels can be used to image the endothelial cells with 300 nm spatial resolutions owing to the photothermal method and with high sensitivity in detecting GNT and deep tissue imaging owing to the photoacoustic method. GNTs have also been applied in a unique detection system for circulating tumor cells devised by Galanzha and colleagues.[64] This system involves using two separate nanoparticles. The tumor cells are first targeted by PEGylated magnetic nanoparticles (MNPs) and GNTs, captured noninvasively in the bloodstream under a magnet, and then verified by rapid photoacoustic detection. This unique multiplexed photoacoustic detection uses the unique properties of the nanomaterials not only for imaging but also for in vivo targeting, magnetic enrichment, signal amplification, and multicolor recognition. Both the MNP made up of a Fe_2O_3 core (commercially obtained) and the GNTs have photoacoustic spectra but at two different wavelengths, 639 nm and 900 nm, respectively. In tumor-bearing mice, this system was able to collect circulating tumor cells by a magnet placed on the skin to collect MNPs and to detect a strong photoacoustic signal coming from the MNPs and GNTs.[64]

AuNPs also have unique molecular imaging capabilities for optical[65] and CT imaging,[66] but these individual capabilities have not yet been applied for multimodal imaging. Molecular-level fluorescent signals can be achieved by unique activation strategies that conjugate fluorophores, peptides, and AuNPs.[65] Owing to the surface plasmon resonance of AuNPs, these nanomaterials can quench fluorescence when in close contact with a fluorophore. In one example, 20 nm AuNPs were conjugated with a Cy5.5-labeled peptide substrate selective for matrix metalloproteinase 2 (MMP-2). This probe had strong quenching properties when the MMP-2 substrate was not digested. In the presence of MMPs, the substrate is digested and the dye is released from the AuNP, giving off a strong fluorescence signal. Such activation has been exemplified in vivo in MMP-2-positive tumor-bearing mice.[67] CT contrast has been achieved by AuNPs, allowing for longer imaging time and reduced toxicity over iodine-based compounds. These AuNPs were coated with PEG to increase circulation lifetime. Owing to the higher atomic number and therefore higher X-ray absorption coefficient than iodine, CT contrast was 5.7 times higher than current iodine-based contrast agents. In addition, in vivo results showed clear differences between cardiac ventricles and great vessels.[66] Such unique imaging capabilities of AuNPs can be applied for multimodality molecular imaging.

Single-walled carbon nanotubes (SWCNTs) are organic materials that can be conceptually seen as a single graphene sheet rolled up into a tubular structure with diameters on the nanoscale. Without the presence of any inorganic materials, and when these nanotubes are well dispersed, SWCNTs exhibit NIR photoluminescence within the 700 to 1,300 nm biologic window,[68,69] strong Raman scattering,[70] and photoacoustic signals[71] that can be

exploited for multimodal imaging with inorganic nanoparticles. Taking advantage of the NIRF emission, O'Connell and colleagues were able to distinguish SWCNTs from biologic systems,[68] and Welsher and colleagues demonstrated the use of SWCNTs stabilized with PEG and targeted to B cells and breast cancer cells as NIRF tags for cell surface probing and imaging.[72] Signature Raman bands for SWCNTs appear at 150 to 300 cm^{-1}, the radial breathing modes, and can be related to the diameter of the nanotubes[73] and at 1,590 to 1,600 cm^{-1}, the G band.[70] Liu and colleagues used Raman spectroscopy to determine the circulation time and biodistribution of SWCNTs functionalized with various lengths of branched and linear PEG by measuring the G-band Raman counts in blood.[74] The photoacoustic signal is also used for detecting and imaging SWNCTs, as seen by De la Zerda and colleagues.[71] Cyclic RGD and PEG conjugated SWCNTs were observed in vivo by the SWCNT intrinsic photoacoustic signal in U87MG tumor–bearing mice.[71] Biodistribution of SWCNT-RGD labeled with ^{64}Cu could also be analyzed in vivo by PET and Raman spectroscopy.[75] Besides the intrinsic properties, Gd doped within SWCNTs can have enhanced effects to the MRI relaxivity. Sitharaman and colleagues loaded ultrashort SWCNTs with nanoscalar, superparamagnetic gadolinium ion (Gd^{3+}) clusters, termed gadonanotubes.[76] These tubes were shown to have 100 times greater MRI T_1-weighted contrast than current Gd^{3+} ion–based clinical contrast agents. This enhancement of paramagnetic relaxation rate of gadonanotubes is due to the nanoscale confinement of Gd^{3+} ions within the carbon capsule sheath. As these individual cases show, carbon nanotubes have potential as multimodal imaging probes by detecting multiple intrinsic and doped material properties.

Other nanoparticles have been combined with NIR photoluminescence probes to produce multimodal molecular imaging probes. IONPs and NIRF SWCNTs encapsulated within oligonucleotides, $d(GT)_{15}$, have been used as MRI-NIRF probes.[77] The IONP used to grow the SWNCTs, $Fe(CO)_5$, attaches to one end of the nanotube during the synthesis. In this MRI-NIRF probe, the SWCNTs act as the NIR fluorophore, the IONP on the end of the tube is the T_2 MRI contrast agent, and the DNA that wraps around the nanotube acts as a stabilizing agent to prevent aggregation and improve biodistribution, as seen in the schematic of Figure 5.[68,69] After SWCNT synthesis, magnetic separation is necessary to select for the IONP-bound SWCNTs. The attachment of the IONP to the SWNT does not reduce the NIR emission of the SWCNTs compared to Fe-enriched and Fe-depleted SWCNTs. Although this nanoparticle was not compared alongside commonly used MRI contrast agents, the combined functionality of SWCNT high-absorbance properties and NIRF emission and the IONP magnetic susceptibility show promise as a new multimodal biomedical imaging agent.[77] These particles were incubated with murine macrophage cells to study the capability of in vitro MR and NIR imaging. MR (see Figure 5B) and NIR (see Figure 5C) imaging were successful with the MRI contrast dependent on the IONP concentration, whereas the NIR emission within the cells was due to SWCNTs present, as verified by the SWCNT signature Raman peaks. No future works have been reported, but with the use of SWCNTs, many targeting groups can be attached for molecular imaging, along with the potential use in therapeutics for tumor ablation by hyperthermia.

SPECT-CT and MRI can provide high-sensitivity and high-resolution imaging if proper contrast agents are used. Lijowski and colleagues developed a targeted nanoparticle that can be detected by sensitive SPECT-CT along with high-resolution MRI.[78] The particle is targeted to integrin $\alpha_n\beta_3$ to characterize tumor angiogenesis with three-dimensional mapping capability. The core of the nanoparticle is radioactive technetium 99m (^{99m}Tc) with functional groups for targeting, and the outer phospholipid layer is made of Gd chelates for MRI. The synthesis of these nanoparticles is initialized by emulsified perfluorooctylbromide. The emulsification includes a surfactant with the integrin-targeted ^{99m}Tc nanoparticles complexed with high-molecular-weight PEG. The surfactant

comixture of the nuclear nanoparticles includes a high molar concentration of Gd diethylenetriaminepentaacetic acid–bis-oleate. The final nanoparticles are emulsified, and these particles were intravenously injected into a Vx2 tumor model in male New Zealand white rabbits. With the use of ^{99m}Tc $\alpha_n\beta_3$ nanoparticles, SPECT-CT produced a neovasculature signal from the tumor that was not seen in the nontumor side. In addition, MR molecular imaging allowed for three-dimensional mapping of angiogenesis in the tumor after the ^{99m}Tc $\alpha_n\beta_3$ nanoparticles were conjugated with Gd nanoparticles. With the use of SPECT-CT and MRI, these particles were able to locate neovasculature around the tumor that was asymmetric and patchy.[78]

The use of rare-earth oxide nanocrystals has been characterized for bimodal fluorescence and paramagnetic imaging of cancer cells.[79] Y_2O_3 nanocrystals doped with Eu^{3+} to show red visible light fluorescence and Gd^{3+} for paramagnetic functionality as MRI contrast agents were also targeted to folate receptor–positive cancer cells by conjugating the cancer targeting ligand folic acid. Y_2O_3 nanocrystals had significant fluorescence quantum efficiency of about 60% and five times greater relaxivity compared to clinically used Gd-based contrast agents when codoped with Eu and Gd, respectively. The development of these nanocrystals, although well developed for use in commercial displays and optical communication, was performed in a wet chemical method for biologic uses. The conjugation scheme of the nanocrystals is seen in Figure 6, where the folic acid is first activated for amine reactivity, then the Eu and Gd doped Y_2O_3 nanocrystals are aminized by polyethylenimine (PEI), and, finally, the amine-reactive folic acid reacts with the PEI nanocrystals to create the folic acid–conjugated nanocrystals. MRI contrast and fluorescence images of the nanocrystal incubated with the folate receptor–positive human nasopharyngeal carcinoma cells are shown in Figure 6.[79] Das and colleagues synthesized Tb-doped and Yb/Er-codoped Gd_2O_3 ultranarrow nanorods that exhibit fluorescence and paramagnetism, leading to good T_1-weighted MRI contrast. [80] The nanorods have diameters at 2.5 nm and lengths at 18.8 nm, which can be attributed to the low cell viability after incubation (about 60%) because larger diameters in the range of 20 to 100 nm have shown more promising biocompatibility and cellular uptake. Although the particles were not used for further in vitro work, fluorescence and MRI signals were possible by the inclusion of rare-earth oxides in a nanorod shape using a single-phase synthesis.

Conclusion

Applications of inorganic nanoparticles continue to advance as more imaging modalities and therapeutic agents are added onto the nanoplatforms. Initial inorganic nanoparticle designs consisted of bare nanoparticles, but as nanotechnology progressed, particles with nuclear-magnetic-fluorescence properties were developed. As advancement continues, biocompatibility, biodistribution, and reproducibility are the main concerns in the development of inorganic nanoparticles. Aggregation and disintegration are the fate of inorganic nanoparticles, and the aggregate or disintegrated nanoparticles can be toxic. Effort is needed to keep their desirable properties intact in physiologic conditions. Not only do these newly developed hybrid nanoparticles need to be nontoxic, but they also must be biocompatible for potential clinical applications. Biocompatibility is defined as the ability of the material to perform biologic function with an appropriate immune response. Further review of the cytotoxicity of all nanomaterials discussed here is found in Lewinski and colleagues.[81] Biocompatibility needs to be understood and studied in a long-term manner before clinical applications are possible. Biodistribution is also an issue, and it is important to understand how these particles are excreted through the body and what organs are being targeted when the particles are delivered. Furthermore, as these nanomaterial imaging agents advance, sophisticated characterization techniques are required to understand if the particle that was intentionally made is still the same particle being injected. Contaminants that may

not have affected previous inorganic material synthesis may now play a critical role in the reproducibility of the particle synthesis. Not only do biocompatibility and biodistribution need to be well understood, but the interactions of all the parts used to develop the materials also have to be studied. More importantly, chronic toxicity and metabolism mechanisms of inorganic nanoparticles in the body need to be revealed.

The recent examples of inorganic nanoparticles as multimodal imaging agents demonstrate the major advantages of engineered nanoparticles. Unique nanoparticle coating, biomolecules, fluorescent dyes, and doped metals can be applied to build bimodal or multimodal imaging probes. Synergistic effects can be achieved among the different molecular imaging agents when combined on nanoplatforms. As nanotechnology progresses and new materials are engineered, the development of multimodal molecular imaging probes will mature in the direction of molecular sensing and therapy, giving doctors and patients the understanding needed to diagnose and treat disease.

References

1. Corot C, Robert P, Idee JM, Port M. Recent advances in iron oxide nanocrystal technology for medical imaging. Adv Drug Deliv Rev. 2006; 58:1471–504.10.1016/j.addr.2006.09.013 [PubMed: 17116343]
2. Medintz IL, Uyeda HT, Goldman ER, Mattoussi H. Quantum dot bioconjugates for imaging, labelling and sensing. Nat Mater. 2005; 4: 435–46.10.1038/nmat1390 [PubMed: 15928695]
3. Barnes WL, Dereux A, Ebbesen TW. Surface plasmon subwavelength optics. Nature. 2003; 424:824–30.10.1038/nature01937 [PubMed: 12917696]
4. Cushing BL, Kolesnichenko VL, O'Connor CJ. Recent advances in the liquid-phase syntheses of inorganic nanoparticles. Chem Rev. 2004; 104:3893–946.10.1021/cr030027b [PubMed: 15352782]
5. Cai W, Chen X. Nanoplatforms for targeted molecular imaging in living subjects. Small. 2007; 3:1840–54.10.1002/smll.200700351 [PubMed: 17943716]
6. Roy I, Ohulchanskyy TY, Bharali DJ, et al. Optical tracking of organically modified silica nanoparticles as DNA carriers: a nonviral, nanomedicine approach for gene delivery. Proc Natl Acad Sci U S A. 2005; 102:279–84.10.1073/pnas.0408039101 [PubMed: 15630089]
7. Sun C, Lee JSH, Zhang MQ. Magnetic nanoparticles in MR imaging and drug delivery. Adv Drug Deliv Rev. 2008; 60:1252–65.10.1016/j.addr.2008.03.018 [PubMed: 18558452]
8. Haynes CL, Van Duyne RP. Nanosphere lithography: a versatile nanofabrication tool for studies of size-dependent nanoparticle optics. J Phys Chem B. 2001; 105:5599–611.10.1021/jp 010657m
9. Hulteen JC, Treichel DA, Smith MT, et al. Nanosphere lithography: size-tunable silver nanoparticle and surface cluster arrays. J Phys Chem B. 1999; 103:3854–63.10.1021/jp9904771
10. Grzelczak M, Perez-Juste J, Mulvaney P, Liz-Marzan LM. Shape control in gold nanoparticle synthesis. Chem Soc Rev. 2008; 37: 1783–91.10.1039/b711490g [PubMed: 18762828]
11. Tao AR, Habas S, Yang P. Shape control of colloidal metal nanocrystals. Small. 2008; 4:310–25.10.1002/smll.200701295
12. Rozenberg BA, Tenne R. Polymer-assisted fabrication of nanoparticles and nanocomposites. Prog Polym Sci. 2008; 33:40–112.10.1016/j.progpolymsci.2007.07.004
13. Jennings LE, Long NJ. 'Two is better than one'—probes for dual-modality molecular imaging. Chem Commun (Camb). 2009; 24: 3511–24.10.1039/b821903f [PubMed: 19521594]
14. Louie A. Multimodality imaging probes: design and challenges. Chem Rev. 2010; 110:3146–95.10.1021/cr9003538 [PubMed: 20225900]
15. Park K, Lee S, Kang E, et al. New generation of multifunctional nanoparticles for cancer imaging and therapy. Adv Funct Mater. 2009; 19:1553–66.10.1002/adfm.200801655
16. Hasegawa BH, Iwata K, Wong KH, et al. Dual-modality Imaging of function and physiology. Acad Radiol. 2002; 9:1305–21.10.1016/S1076-6332(03)80564-0 [PubMed: 12449363]
17. Na HB, Song IC, Hyeon T. Inorganic nanoparticles for MRI contrast agents. Adv Mater. 2009; 21:2133–48.10.1002/adma. 200802366

18. Marckmann P, Skov L, Rossen K, et al. Nephrogenic systemic fibrosis: suspected causative role of gadodiamide used for contrast-enhanced magnetic resonance imaging. J Am Soc Nephrol. 2006; 17: 2359–62.10.1681/ASN.2006060601 [PubMed: 16885403]
19. Lee JH, Huh YM, Jun Y, et al. Artificially engineered magnetic nanoparticles for ultra-sensitive molecular imaging. Nat Med. 2007; 13:95–9.10.1038/nm1467 [PubMed: 17187073]
20. Josephson L, Kircher MF, Mahmood U, et al. Near-infrared fluorescent nanoparticles as combined MR/optical imaging probes. Bioconjug Chem. 2002; 13:554–60.10.1021/bc015555d [PubMed: 12009946]
21. Kircher MF, Allport JR, Graves EE, et al. In vivo high resolution three-dimensional imaging of antigen-specific cytotoxic T-lymphocyte trafficking to tumors. Cancer Res. 2003; 63:6838–46. [PubMed: 14583481]
22. Santra S, Kaittanis C, Grimm J, Perez JM. Drug/dye-loaded, multifunctional iron oxide nanoparticles for combined targeted cancer therapy and dual optical/magnetic resonance imaging. Small. 2009; 5:1862–8.10.1002/smll.200900389 [PubMed: 19384879]
23. Chen K, Xie J, Xu HY, et al. Triblock copolymer coated iron oxide nanoparticle conjugate for tumor integrin targeting. Biomaterials. 2009; 30:6912–9.10.1016/j.biomaterials.2009. 08.045 [PubMed: 19773081]
24. Cai W, Chen X. Multimodality molecular imaging of tumor angiogenesis. J Nucl Med. 2008; 49(Suppl 2):113S–28S.10.2967/ jnumed.107.045922 [PubMed: 18523069]
25. Romberg B, Hennink WE, Storm G. Sheddable coatings for long-circulating nanoparticles. Pharm Res. 2008; 25:55–71.10.1007/ s11095-007-9348-7 [PubMed: 17551809]
26. Jayagopal A, Russ PK, Haselton FR. Surface engineering of quantum dots for in vivo vascular imaging. Bioconjug Chem. 2007; 18:1424–33.10.1021/bc070020r [PubMed: 17760416]
27. Chen H, Wang L, Yeh J, et al. Reducing non-specific binding and uptake of nanoparticles and improving cell targeting with an antifouling PEO-b-PgammaMPS copolymer coating. Biomaterials. 2010; 31:5397–407.10.1016/j.biomaterials.2010.03.036 [PubMed: 20398933]
28. Choi JS, Park JC, Nah H, et al. A hybrid nanoparticle probe for dual-modality positron emission tomography and magnetic resonance imaging. Angew Chem Int Ed Engl. 2008; 47:6259–62.10.1002/anie.200801369 [PubMed: 18613191]
29. Wang YX, Hussain SM, Krestin GP. Superparamagnetic iron oxide contrast agents: physicochemical characteristics and applications in MR imaging. Eur Radiol. 2001; 11:2319–31.10.1007/s003300 100908 [PubMed: 11702180]
30. Lee HY, Li Z, Chen K, et al. PET/MRI dual-modality tumor imaging using arginine-glycine-aspartic (RGD)-conjugated radiolabeled iron oxide nanoparticles. J Nucl Med. 2008; 49:1371–9.10.2967/jnumed.108.051243 [PubMed: 18632815]
31. Choi SH, Na BH, Il Park YI, et al. Simple and generalized synthesis of oxide-metal heterostructured nanoparticles and their applications in multimodal biomedical probes. J Am Chem Soc. 2008; 130: 15573–80.10.1021/ja805311x [PubMed: 18950167]
32. Wang C, Irudayaraj J. Multifunctional magnetic-optical nanoparticle probes for simultaneous detection, separation, and thermal ablation of multiple pathogens. Small. 2010; 6:283–9.10.1002/smll.200901596 [PubMed: 19943255]
33. Xu C, Xie J, Ho D, et al. Au-Fe3O4 dumbbell nanoparticles as dual-functional probes. Angew Chem Int Ed Engl. 2008; 47:173–6.10.1002/anie.200704392 [PubMed: 17992677]
34. Xie J, Chen K, Huang J, et al. PET/NIRF/MRI triple functional iron oxide nanoparticles. Biomaterials. 2010; 31:3016–22.10.1016/ j.biomaterials.2010.01.010 [PubMed: 20092887]
35. Alivisatos AP. Semiconductor clusters, nanocrystals, and quantum dots. Science. 1996; 271:933–7.10.1126/science.271.5251.933
36. Michalet X, Pinaud FF, Bentolila LA, et al. Quantum dots for live cells, in vivo imaging, and diagnostics. Science. 2005; 307:538–44.10.1126/science.1104274 [PubMed: 15681376]
37. Biju V, Itoh T, Ishikawa M. Delivering quantum dots to cells: bioconjugated quantum dots for targeted and nonspecific extracellular and intracellular imaging. Chem Soc Rev. 2010; 39:3031–56. [PubMed: 20508886]
38. Gao J, Chen X, Cheng Z. Near-infrared quantum dots as optical probes for tumor imaging. Curr Top Med Chem. 2010; 10:1147–57. [PubMed: 20388111]

39. Bentolila LA, Ebenstein Y, Weiss S. Quantum dots for in vivo small-animal imaging. J Nucl Med. 2009; 50:493–6.10.2967/ jnumed.108.053561 [PubMed: 19289434]
40. Mulder WJ, Koole R, Brandwijk RJ, et al. Quantum dots with a paramagnetic coating as a bimodal molecular imaging probe. Nano Lett. 2006; 6:1–6.10.1021/nl051935m [PubMed: 16402777]
41. Koole R, van Schooneveld MM, Hilhorst J, et al. Paramagnetic lipid-coated silica nanoparticles with a fluorescent quantum dot core: a new contrast agent platform for multimodality imaging. Bioconjug Chem. 2008; 19:2471–9.10.1021/bc800368x [PubMed: 19035793]
42. Xie R, Kolb U, Li J, et al. Synthesis and characterization of highly luminescent CdSe–Core CdS/ Zn0.5Cd0.5S/ZnS multishell nanocrystals. J Am Chem Soc. 2005; 127:7480–8.10.1021/ja042939g [PubMed: 15898798]
43. Kirchner C, Liedl T, Kudera S, et al. Cytotoxicity of colloidal CdSe and CdSe/ZnS nanoparticles. Nano Lett. 2005; 5:331–8.10.1021/ nl047996m [PubMed: 15794621]
44. Tu C, Ma X, Pantazis P, et al. Paramagnetic, silicon quantum dots for magnetic resonance and two-photon imaging of macrophages. J Am Chem Soc. 2010; 132:2016–23.10.1021/ja909303g [PubMed: 20092250]
45. Lim YT, Cho MY, Kang JH, et al. Perfluorodecalin/InGaP/ZnS quantum dots nanoemulsions as F-19 MR/optical imaging nanoprobes for the labeling of phagocytic and nonphagocytic immune cells. Biomaterials. 2010; 31:4964–71.10.1016/j.biomaterials. 2010.02.065 [PubMed: 20346494]
46. Shashkov EV, Everts M, Galanzha EI, Zharov VP. Quantum dots as multimodal photoacoustic and photothermal contrast agents. Nano Lett. 2008; 8:3953–8.10.1021/nl802442x [PubMed: 18834183]
47. Berciaud S, Cognet L, Lounis B. Photothermal absorption spectroscopy of individual semiconductor nanocrystals. Nano Lett. 2005; 5:2160–3.10.1021/nl051805d [PubMed: 16277445]
48. Akerman ME, Chan WC, Laakkonen P, et al. Nanocrystal targeting in vivo. Proc Natl Acad Sci U S A. 2002; 99:12617–21.10.1073/ pnas.152463399 [PubMed: 12235356]
49. Dubertret B, Skourides P, Norris DJ, et al. In vivo imaging of quantum dots encapsulated in phospholipid micelles. Science. 2002; 298:1759–62.10.1126/science.1077194 [PubMed: 12459582]
50. Larson DR, Zipfel WR, Williams RM, et al. Water-soluble quantum dots for multiphoton fluorescence imaging in vivo. Science. 2003; 300:1434–6.10.1126/science.1083780 [PubMed: 12775841]
51. Gao X, Cui Y, Levenson RM, et al. In vivo cancer targeting and imaging with semiconductor quantum dots. Nat Biotechnol. 2004; 22:969–76.10.1038/nbt994 [PubMed: 15258594]
52. Kim S, Lim YT, Soltesz EG, et al. Near-infrared fluorescent type II quantum dots for sentinel lymph node mapping. Nat Biotechnol. 2004; 22:93–7.10.1038/nbt920 [PubMed: 14661026]
53. Cai W, Chen K, Li ZB, et al. Dual-function probe for PET and near-infrared fluorescence imaging of tumor vasculature. J Nucl Med. 2007; 48:1862–70.10.2967/jnumed.107.043216 [PubMed: 17942800]
54. Caruso F, Caruso RA, Mohwald H. Nanoengineering of inorganic and hybrid hollow spheres by colloidal templating. Science. 1998; 282:1111–4.10.1126/science.282.5391.1111 [PubMed: 9804547]
55. Rieter WJ, Kim JS, Taylor KM, et al. Hybrid silica nanoparticles for multimodal imaging. Angew Chem Int Ed Engl. 2007; 46:3680–2.10.1002/anie.200604738 [PubMed: 17415734]
56. Loo C, Lowery A, Halas N, et al. Immunotargeted nanoshells for integrated cancer imaging and therapy. Nano Lett. 2005; 5:709–11.10.1021/nl050127s [PubMed: 15826113]
57. Chen J, Wang D, Xi J, et al. Immuno gold nanocages with tailored optical properties for targeted photothermal destruction of cancer cells. Nano Lett. 2007; 7:1318–22.10.1021/nl070345g [PubMed: 17430005]
58. Huang X, El-Sayed IH, Qian W, El-Sayed MA. Cancer cell imaging and photothermal therapy in the near-infrared region by using gold nanorods. J Am Chem Soc. 2006; 128:2115–20.10.1021/ ja057254a [PubMed: 16464114]
59. Bohren, CF.; Huffman, DF. Absorption and scattering of light by small particles. New York: Wiley; 1983.

60. Boyer D, Tamarat P, Maali A, et al. Photothermal imaging of nanometer-sized metal particles among scatterers. Science. 2002; 297:1160–3.10.1126/science.1073765 [PubMed: 12183624]
61. Wang, L., editor. Photoacoustic imaging and spectroscopy. New York: CRC Press; 2009.
62. Bardhan R, Chen W, Perez-Torres C, et al. Nanoshells with targeted simultaneous enhancement of magnetic and optical imaging and photothermal therapeutic response. Adv Funct Mater. 2009; 19:3901–9.10.1002/adfm.200901235
63. Kim JW, Galanzha EI, Shashkov EV, et al. Golden carbon nanotubes as multimodal photoacoustic and photothermal high-contrast molecular agents. Nat Nanotechnol. 2009; 4:688–94.10.1038/nnano.2009.231 [PubMed: 19809462]
64. Galanzha EI, Shashkov EV, Kelly T, et al. In vivo magnetic enrichment and multiplex photoacoustic detection of circulating tumour cells. Nat Nanotechnol. 2009; 4:855–60.10.1038/nnano.2009.333 [PubMed: 19915570]
65. Lee S, Park K, Kim K, et al. Activatable imaging probes with amplified fluorescent signals. Chem Commun (Camb). 2008; 36:4250–60. [PubMed: 18802536]
66. Kim D, Park S, Lee JH, et al. Antibiofouling polymer-coated gold nanoparticles as a contrast agent for in vivo x-ray computed tomography imaging. J Am Chem Soc. 2007; 129:7661–5.10. 1021/ja071471p [PubMed: 17530850]
67. Lee S, Cha EJ, Park K, et al. A near-infrared-fluorescence-quenched gold-nanoparticle imaging probe for in vivo drug screening and protease activity determination. Angew Chem Int Ed Engl. 2008; 47: 2804–7.10.1002/anie.200705240 [PubMed: 18306196]
68. O'Connell MJ, Bachilo SM, Huffman CB, et al. Band gap fluorescence from individual single-walled carbon nanotubes. Science. 2002; 297:593–6.10.1126/science.1072631 [PubMed: 12142535]
69. Wray S, Cope M, Delpy DT, et al. Characterization of the near infrared absorption spectra of cytochrome aa3 and haemoglobin for the non-invasive monitoring of cerebral oxygenation. Biochim Biophys Acta. 1988; 933:184–92.10.1016/0005-2728(88)90069-2 [PubMed: 2831976]
70. Satio, R.; Dresselhaus, G.; Dresselhaus, MS. Physical properties of carbon nanotubes. London: Imperial College Press; 1998.
71. De la Zerda A, Zavaleta C, Keren S, et al. Carbon nanotubes as photoacoustic molecular imaging agents in living mice. Nat Nanotechnol. 2008; 3:557–62.10.1038/nnano.2008.231 [PubMed: 18772918]
72. Welsher K, Liu Z, Daranciang D, Dai H. Selective probing and imaging of cells with single walled carbon nanotubes as near-infrared fluorescent molecules. Nano Lett. 2008; 8:586–90.10. 1021/nl072949q [PubMed: 18197719]
73. Dresselhaus MS, Dresselhaus G, Saito R, Jorio A. Raman spectroscopy of carbon nanotubes. Phys Rep. 2005; 409:47–99.10.1016/j.physrep.2004.10.006
74. Liu Z, Davis C, Cai W, et al. Circulation and long-term fate of functionalized, biocompatible single-walled carbon nanotubes in mice probed by Raman spectroscopy. Proc Natl Acad Sci U S A. 2008; 105:1410–5.10.1073/pnas.0707654105 [PubMed: 18230737]
75. Zavaleta C, De la Zerda A, Liu Z, et al. Noninvasive Raman spectroscopy in living mice for evaluation of tumor targeting with carbon nanotubes. Nano Lett. 2008; 8:2800–5.10.1021/nl801362a [PubMed: 18683988]
76. Sitharaman B, Kissell KR, Hartman KB, et al. Superparamagnetic gadonanotubes are high-performance MRI contrast agents. Chem Commun (Camb). 2005; 31:3915–7.10.1039/b504435a [PubMed: 16075070]
77. Choi JH, Nguyen FT, Barone PW, et al. Multimodal biomedical imaging with asymmetric single-walled carbon nanotube/iron oxide nanoparticle complexes. Nano Lett. 2007; 7:861–7.10. 1021/nl062306v [PubMed: 17335265]
78. Lijowski M, Caruthers S, Hu G, et al. High sensitivity high-resolution SPECT-CT/MR molecular imaging of angiogenesis in the Vx2 model. Invest Radiol. 2009; 44:15–22.10.1097/RLI.0b013e31818935eb [PubMed: 18836386]
79. Setua S, Menon D, Asok A, et al. Folate receptor targeted, rare-earth oxide nanocrystals for bi-modal fluorescence and magnetic imaging of cancer cells. Biomaterials. 2010; 31:714–29.10.1016/j.biomaterials.2009.09.090 [PubMed: 19822364]

80. Das GK, Heng BC, Ng SC, et al. Gadolinium oxide ultranarrow nanorods as multimodal contrast agents for optical and magnetic resonance imaging. Langmuir. 2010; 26:8959–65.10.1021/la904751q [PubMed: 20148548]

81. Lewinski N, Colvin V, Drezek R. Cytotoxicity of nanoparticles. Small. 2008; 4:26–49.10.1002/smll.200700595 [PubMed: 18165959]

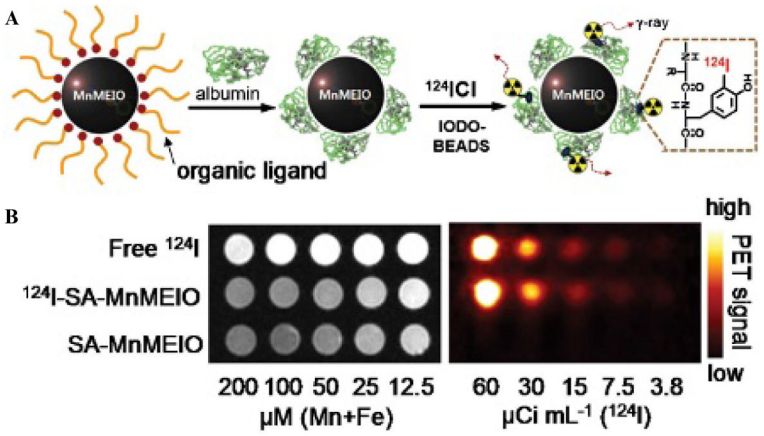

Figure 1.

A, Schematic of the functionalization of manganese-based magnetic engineered iron oxide (MnMEIO) with serum albumin (SA) and the isotope ^{124}I-SA. *B*, The stronger-intensity MR (*left*) and PET (*right*) signals are seen here with the use of the bimodal imaging agent as opposed to a free isotope or free iron oxide particle. Adapted from Choi JS et al.[28]

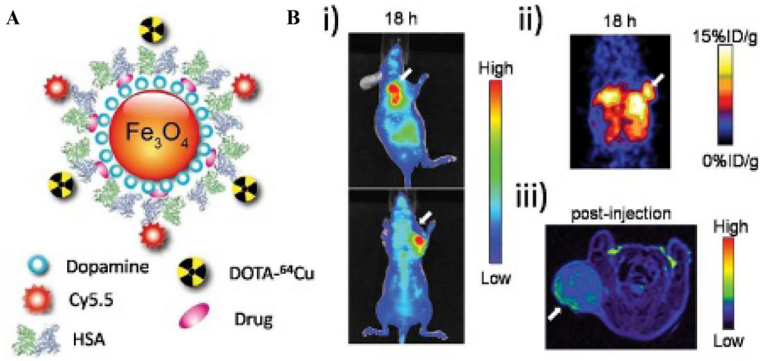

Figure 2.

A, Iron oxide nanoparticles coated with human serum albumin (HSA), ^{64}Cu-DOTA, and Cy5.5 allow for MRI, PET, and NIRF imaging. *B*, In vivo mice (i) NIRF, (ii) PET, and (iii) MR images of the particle 18 hours postinjection. Adapted from Xie J et al.[34]

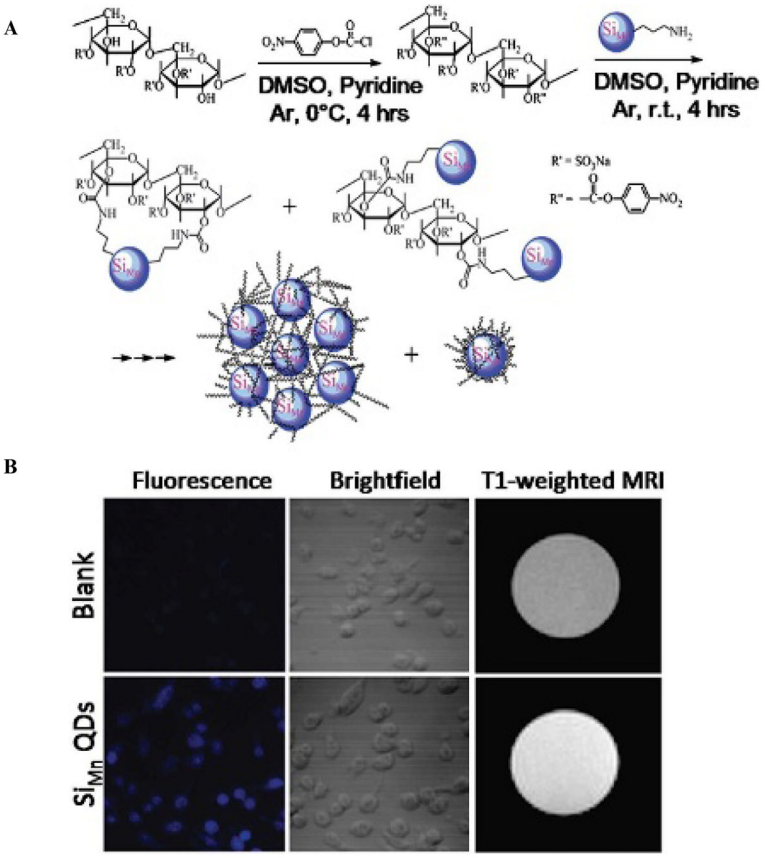

Figure 3.

A, Schematic of the synthesis of dextran sulfate–coated Mn-doped SiQDs that exhibit fluorescence and strong T_1 MRI contrast. *B*, Confocal imaging and T_1-weighted MRI of blank mouse macrophages and ones incubated with dextran sulfate–coated Mn-doped QDs. Adapted from Tu C et al.[44] DMSO = dimethylsulfoxide.

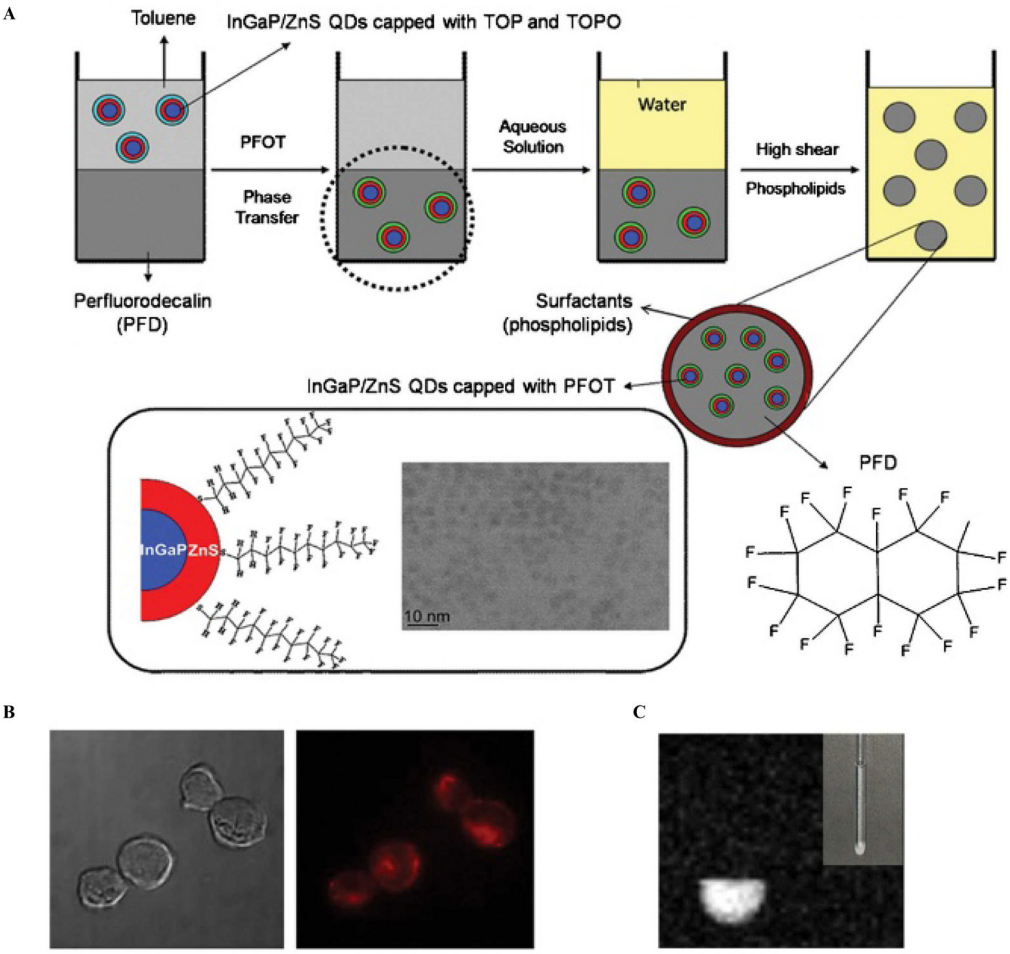

Figure 4.

A, Schematic diagram of the synthesis of the PFD/[InGaP/ZnS QDs] nanoemulsions. The InGaP/ZnS QDs dispersed in PFD were observed using transmission electron microscopy. *B*, Fluorescence images of NK92MI cells that have taken up PFD/[InGaP/ZnS QDs] nanoemulsions without the use of transfecting agents. The fluorescence emission signal is due to the InGaP/ZnS QDs. *C*, ^{19}F-based MRIof NK92MI cells labeled with the nanoemulsions giving off a strong MR signal owing to the presence of perfluorocarbons. Adapted from Lim YT et al.[45] PFOT = perfluorooctanethiol; TOP = tri-n-octylphosphine; TOPO = tri-n-octylphosphineoxide.

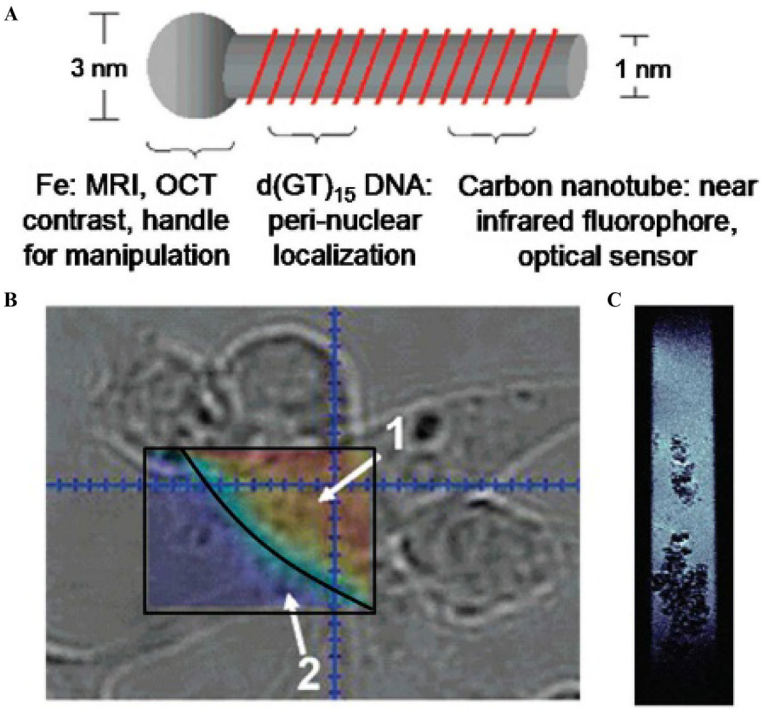

Figure 5.

A, Schematic of the DNA-wrapped nanotube iron oxide nanoparticle complex. *B*, NIR image at the cell boundary of macrophages after being incubated with Fe-enriched SWNT. The area within the box labeled (1) correlates to the interior of the cell and corresponds to a high SWNT concentration. The area labeled (2) indicates a low NIR signal, meaning that no SWNTs were found outside the cell boundary. *C*, T_2-weighted MRI of macrophage cells incubated with the Fe-enriched SWNT. As IONPs are T_2 contrast agents, the negative contrast is verified by the dark areas within the cells. The cells were incubated in cell media for 7 hours with 10 mg/mL Fe-SWNT. The image was produced using a T_2-weighted spin echo multi-slice sequence with a pulse repetition time of 1.2 seconds and an echo time of 10 milliseconds. Adapted from Choi JH et al.[77]

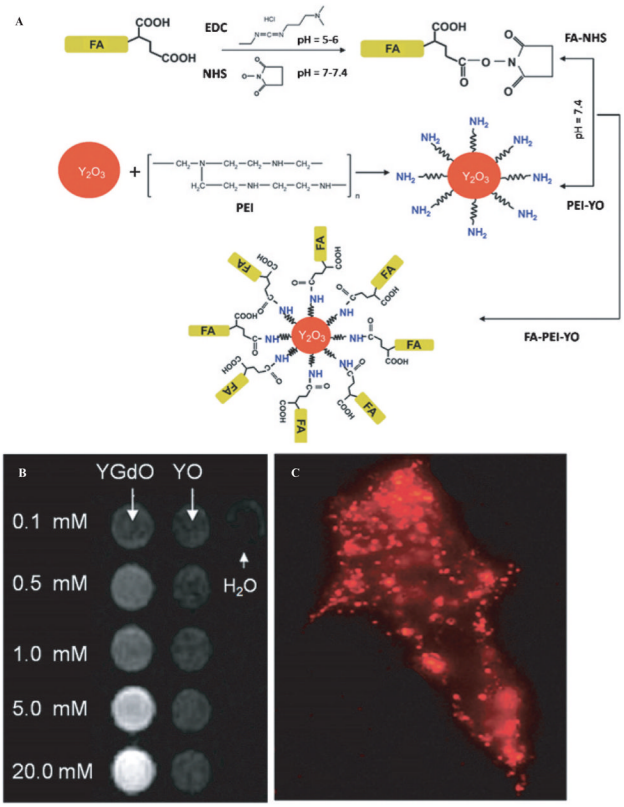

Figure 6.

A, Scheme of the conjugation of folic acid to the fluorescent Eu- and paramagnetic Gd-doped Y_2O_3 nanocrystals. *B*, T_1-weighted spin echo pulse sequence MRI at 1.5 T of the Gd-doped nanocrystals (YGdO) versus the undoped nanocrystals (YO) at different concentrations. *C*, Dark-field fluorescent image of folate receptor–positive human nasopharyngeal carcinoma cells incubated with 2 mM of Eu- and Gd-doped Y2O3 nanocrystals for 4 hours. Adapted from Setua S et al.[79] EDC = 1-ethyl-3-[3-dimethylaminopropyl] carbodiimide hydrochloride; FA = folic acid.